

PARTICLE TRANSPORT-DRIVEN FLOW MODULATION IN SOLAR PHOTOVOLTAIC MODULES

Sarah E. Smith

Department of Mechanical and Materials Engineering.
Portland State University
Portland, OR 97215
smith33@pdx.edu

Marc Calaf

Department of Mechanical Engineering
University of Utah
Salt Lake City, UT 84112
marc.calaf@utah.edu

Raúl Bayoán Cal

Department of Mechanical and Materials Engineering.
Portland State University
Portland, OR 97215
rcal@pdx.edu

Henda Djeridi

Université Grenoble - Alpes
Grenoble, France F-38000
Henda.Djeridi@legi.grenoble-inp.fr

Martin Obligado

Université Grenoble - Alpes
Grenoble, France F-38000
Martin.Obligado@univ-grenoble-alpes.fr

ABSTRACT

Particle-laden flows in solar photovoltaic (PV) systems are inevitable, where wind-swept debris in open environments are carried by high winds and turbulence, coating panel surfaces or damaging structures. Particle deposition, or soiling, is a well-known issue for large-scale plants which rely on uninhibited solar rays for optimal production. But understanding the mechanisms leading to soiling requires a physical and fluid dynamics-centered focus, since turbulence dominates PV panel wakes and is also known to alter particle concentration and trajectories. This study presents an experimental campaign toward consequences of particle-laden flow between two model PV panels using time-resolved particle image velocimetry. The model array was subjected to varied particle volume fractions (ϕ_v), including a tracer particle case and a water droplet case. Characterization of mean velocity and turbulence statistics within the single phase and, separately, particle phase flows showed modified features due to particle inertia. Images captured at a frequency of 1 kHz in the near wake of the upstream panel allow for a first experimental look at the flow field for single-phase and particle-phase flows which are crucial to debris transport and soiling in PV environments.

INTRODUCTION

In the canopy flow of large-scale solar photovoltaic (PV) systems, turbulent dynamics dominate debris trajectories. Wind interactions with panel structures induce compounding wakes and regions where air is drafted into and out of the plant per Stanislawski *et al.* (2022). In the open regions often inhabited by PV plants, these winds also tend to propel dusts, sands and even larger particles which deposit on panel surfaces and limit efficiency shown by Janiere Silva de

Souza *et al.* (2022) or induce structural damage such as surface abrasion and cracking as in Miller *et al.* (2016). For even relatively moderate conditions, particle deposition on panel surfaces (*i.e.* soiling) limits necessary light and creates cell-damaging hotspots, accounting for efficiency losses more than 30% reported in Zaihidee *et al.* (2016) and on the order of 11% per month, demonstrated in Said (1990), in some cases for large-scale PV systems. In more turbulent environments and stronger winds, enhanced capture and propulsion of larger material increases physical loading impacts as shown in Thornton (1992) as well as deposition rates based on relative forcing between the particles and panel surfaces reported by Moutinho *et al.* (2017). Desert regions, for example, are particularly susceptible to vortical convective updrafts, known as “dust devils”, which can reach storm-like wind speeds while lifting and propelling debris along their path per Rafkin *et al.* (2016).

This manuscript represents the first of its kind to highlight particle-laden turbulence in PV panel near wakes while focusing on turbulence-induced flow dependence on particle presence. In this study we examine the near wake between two model PV panels subjected to polydisperse water droplets (*i.e.* inertial particles) as compared to neutrally-buoyant tracers. As the work presented in Smith *et al.* (2023) considered particle-laden wake effects from the perspective of a downstream panel, this zoomed-in perspective on the near wake of the upstream panel allows for a more focused understanding of wake mechanics through increased spatial resolution and vorticity characterization. In total, this study thus informs on the primary mechanisms leading to particle transport and soiling by introducing a new type of analysis which focuses on fundamental coupling of particles in vortex-dominated PV panel wakes.

EXPERIMENTAL SETUP

Experiments were performed in the closed-loop Lespinard wind tunnel at Laboratoire des Ecoulements Geophysique et Industriel (LEGI) in Grenoble, France. The tunnel, with cross-section of 0.75×0.75 m and a test section 5 m long (Figure 1), is capable of producing wind speeds from 2–45 m/s. For the accompanying experiments, two subsequent passive grid systems at the tunnel inlet produced low turbulence upon interaction with the inflow. First, a grid system of rotating metal winglets, separated a distance of 10 cm in the vertical and horizontal directions, were held stationary in the ‘open’ position with all winglets set parallel to the incoming flow. The grid generates a turbulence intensity of 2–3%. Positioned 12 cm downstream from the winglet grid, a grid of 36 water spray nozzles, also separated 10×10 cm apart, was centered with respect to the tunnel cross-section.

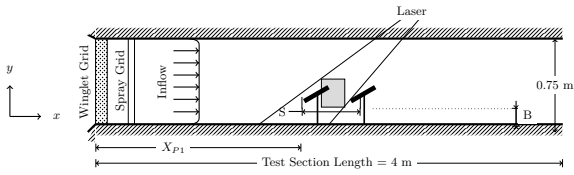


Figure 1. Schematic of wind tunnel facility, module arrangement, and PIV laser sheet positioning. Panels were set at lower panel edge height $B = 310$ mm, and with panel separation of $S = 1.7L_p$

The 0.4 mm diameter nozzles produced polydisperse droplets 26 to 45 μm in diameter, with Stokes numbers (St) ranging between $St = 0.1$ to 2.17 as in Ferran *et al.* (2023). Droplet flow rate for the water particle case was adjusted by external regulator as a volumetric flow rate (L/min) supplied to the spray grid. In the present discussion, the flow rate of 2 L/min corresponds to inflow volume fraction of $\phi_{v,2} = V_p/V_{total} = 2.1 \times 10^{-5}$, where V_p represents the volume of water introduced into the tunnel and V_{total} as the combined volume of air and particles entering the cross-section. The density of the water droplets (ρ_p) compared to that of air (ρ_{air}) was on the order of 800, mimicking common bulk densities of silt and organic matter USDA (2012). The particle concentration of $\phi_{v,0} = 0$ here represents the experimental case where only nearly neutrally buoyant tracer particles were inserted into the tunnel flow using an Antari Alpha F-80Z fog machine, which produced vapor particles by heating a water-glycol mixture. Inflow air velocity for all cases was set to 2.8 m/s, with single-phase flow turbulence intensity measurements on the order of 2.8% in accordance with studies performed by Mora *et al.* (2019) in the same facility.

Panel Models: Design and Placement

The model array consisted of two panel analogs whose construction was based on those in the wind tunnel studies of Glick *et al.* (2020a). Panel dimensions were set at a scaled ratio of 6:1 compared to the small array experiment modules, with panel length of $L_p = 305$ mm representing approximately 1:6 scaling in terms of industrial PV panel length. Each panel was 15 mm thick and comprised 4 layers from front surface to rear. Two 6 mm thick aluminum plates acted as panel front and back surfaces, with area dimensions of $L_p = 305 \times W_p = 609$ mm. Under the front plate, two side-by-side kapton heaters

covering the panel area imposed an evenly distributed and constant heat flux ($\approx 450 \text{ W/m}^2$), mimicking the adverse thermal behavior of desert systems as shown in Smith *et al.* (2023). Between the heater and the rear surface, a layer of aerogel insulation was placed to impose and observe variations in front and rear module heating with respect to the two surfaces. For all cases considered in this discussion, the panels were set with first panel (P_1) at a downstream distance of $x = 2090$ mm from the spray grid and the second panel (P_2) set at $x = 2614$ mm, corresponding to a separation between the two panels of $S = 1.7L_p$. The modules were set to heights of $B = 310$ mm from the tunnel floor with inclination angle of 30° .

Particle Image Velocimetry

Flow measurements were captured with particle image velocimetry (PIV) within the wake of P_1 . In this process, planar images of particles are taken within the wake region at discrete time steps and velocity fields are calculated by translating particle motion in a pixelated field to the accompanying relative space. Images in the present experiments were captured using a Phantom V2640 4M camera equipped with a Zeiss Milvus 2/50M lens. This camera model is capable of capturing images at 6,600 frames per second with a resolution of 2048×1920 pixels. Flow field illumination was produced by a LD-527 Litron Pulsed ND:YLF Laser, with firing repetition rates between 0.2 and 20 kHz, at a wavelength of 527 nm and optimal output energy of 30 mJ at 1kHz. The laser produced a light sheet in the x - y plane which entered the tunnel at a 30° angle to optimize for illumination underneath and behind P_1 as shown in Figure 1. Laser plane alignment coincided with a calibration plate centered 2400 mm downstream of the inlet, with planar orientation measured within $\pm 1^\circ$ of horizontal and vertical axes. The camera was situated outside of the tunnel, with the field of view positioned perpendicular to the laser sheet and encompassing 368 mm and 351 mm in the x and y directions, respectively. Image resolution within the plane spanned 2048×1952 pixels with a resulting in-plane scaling of 5.6 pixels/mm. Simultaneous camera frame rate and laser pulse rate were governed *via* the Dantec Dynamics Synchronizer system controlled through Dynamic Studio software. Each campaign collected a minimum of 2000 double-frame snapshot sets at a firing rate of 1 kHz, where time between the double frame exposures was set to $\Delta t = 100 \mu\text{s}$.

For the $\phi_{v,0}$ tracer case, image processing considered the nearly neutrally-buoyant tracer vapor particles. In the inertial particle case, PIV processing was based on the water droplets and the resulting velocity fields correspond to particle dynamics rather than that of the air, both of which are expected to be different due to coupling and interplay between the two phases. While not the same as the carrier phase, particle velocity fields are valuable information for two reasons. First, the particle behavior is what ultimately controls deposition in the panels, and second, the particle velocity fields are useful inputs for future numerical simulations and theoretical modelling. Processing in Dynamic Studio between each double-frame set was based on particle displacement within decreasing interrogation windows of 32×32 and 16×16 pixels, resulting in vector fields of 128×122 grid points with a resolution of 2.9 mm/point. Vectors whose spatio-temporal correlations were less than 0.3 and/or had a peak height ratio of less than 1.8 were filtered and replaced by nearest neighbor interpolation in post-processing.

RESULTS

Figures 2 and 3 include contours of all time-averaged mean flow and turbulence statistics, respectively, in the wake

of the upstream panel P_1 . The upper row of each contour set represents tracer flow ($\phi_{v,0}$), and the bottom represents presence of inertial particles ($\phi_{v,2}$). In all presented frames, streamwise flow is moving from left-to-right, and empty (*i.e.* white) regions are locations where obstructions such as panel presence, shadows, and/or reflections limited particle visibility.

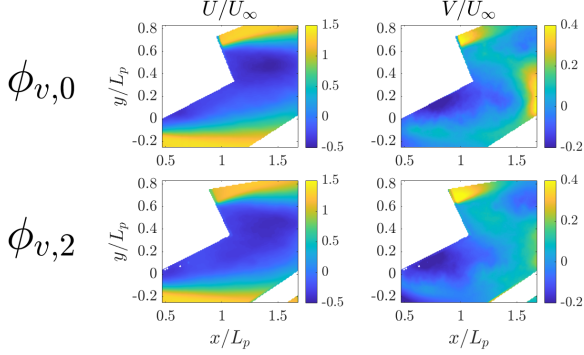


Figure 2. Time-averaged velocity in P_1 wake, normalized with respect to inflow (U_∞). Left to right: streamwise (U/U_∞) and vertical velocity (V/U_∞); Top: tracer flow, Bottom: water particles at $\phi_{v,2}$

The leftmost contours in Figure 2 show time-averaged streamwise velocity ($U = \bar{u}$) as normalized by the freestream (U/U_∞). The smaller wake width in the tracer case, compared to $\phi_{v,2}$, demonstrates higher velocity flow above and below the panel profile, where accompanied particle inertia of $\phi_{v,2}$ prohibits forward motion, especially below the lower panel edge. In the contours for normalized mean vertical velocity V/U_∞ , positive values represent upward motion. For both cases, two lobes of increased downward velocity are visible in the panel wake profile and in the upper region downstream, as also observed in Smith *et al.* (2023). At the top edge of downstream location the wake profile, particles initially launched upward over the panel begin to fall near the region of $x = 1.5L$. In the $\phi_{v,0}$ case, the negative V/U_∞ behavior directly behind the panel is a signature of flow being entrained into the re-circulation region behind the panel surface, as observed from the immediate downward velocity leaving the panel trailing edge. The enhancement of visible downward trajectories in the $\phi_{v,2}$ case observed in the bottom half of the panel profile are due to interaction with the lower panel edge, where particle motion is interrupted by panel interaction and gravitational effects begin to prevail. However, the commonalities in general contour shape and near wake behavior of U/U_∞ and V/U_∞ between the tracer and inertial particles, especially near the upper panel edge, suggests that the effect of hydrodynamic forcing (*e.g.* history, drag, lift, etc.) is more influential than gravitational effects. In terms of PV soiling, this feature, along with the enhancement of downward flow and slower streamwise velocity panel wake together represent ideal conditions for downstream panel deposition.

Contours in Figure 3 represent turbulent Reynolds stresses for the panel wake. Here the leftmost contour of $\overline{u'v'}$ represents, for the carrier phase, turbulence production within the panel wake. A positive quantity denotes that both fluctuations u' and v' have the same sign. Thus, a positive value of $\overline{u'v'}$ indicates either simultaneous upward and streamwise, or downward and reversed fluctuations.

Conversely, negative values indicate opposing signs and

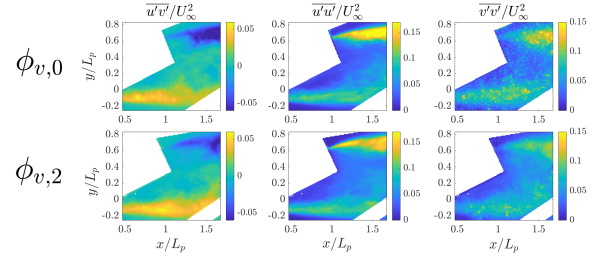


Figure 3. Time-averaged turbulence statistics in the wake of P_1 , normalized with respect to inflow velocity U_∞ . Left to right: Reynolds stresses $\overline{u'v'}/U_\infty^2$, $\overline{u'u'}/U_\infty^2$, and $\overline{v'v'}/U_\infty^2$; Top: tracer flow, Bottom: water particles at $\phi_{v,2}$

represent either simultaneous streamwise and downward or reversed and upward direction. The two lobes visible in each contour are typical arrangements for wake flow, however their asymmetrical positioning is due to the inclined panel Chen & Fang (1996). The overall shape of these lobes mimic each other for $\phi_{v,0}$ and $\phi_{v,2}$. However, magnitudes of $\overline{u'v'}/U_\infty^2$ for $\phi_{v,0}$ are intensified compared to $\phi_{v,2}$, highlighting turbulence production of the tracer flow, where dampening for $\phi_{v,2}$ is again a feature of the particle inertia affecting particle trajectories. The normal stress term $\overline{u'u'}/U_\infty$ is typically enhanced when accompanying flow separation within wake regions generates turbulent momentum in the mean flow direction. In both ϕ_v cases, $\overline{u'u'}/U_\infty$ is greatest above and below the wake profile, where the flow detaches after interacting with the panel edges. The vertical stress term $\overline{v'v'}$ represents vertical momentum induced by turbulence within the wake. For both normal stresses, the particles in $\phi_{v,2}$ dampen the turbulent effects in the panel wake, especially at the upper wake edge. Together with the mean velocity contours U/U_∞ and V/U_∞ , the diminished turbulence and enhanced gravitational effects due to particle presence point to inhibition of inertial particles to precisely follow the flow field compared to tracers.

CONCLUSIONS

The present study investigated behavior of inertial particles ($\phi_{v,2}$) in the asymmetric wake of a model PV panel, compared to that of neutrally buoyant tracers ($\phi_{v,0}$), with a specific focus on mean and turbulent flow statistics. The $\phi_{v,2}$ case showed a broader wake width than $\phi_{v,0}$, with slower mean streamwise velocity (U) and increased downward velocity (V) stemming from interactions with the lower panel edge, where particle motion is interrupted, and gravitational effects become dominant. Additionally, minimized Reynolds stresses for $\phi_{v,2}$ compared to $\phi_{v,0}$ were observed along the wake profile, pointing to characteristic turbulence-dampening effects of partial inertia in the particle-laden case.

In total, the results emphasize the influence of particle inertia on flow behavior for PV arrays. The combination of dampened mean velocity and turbulence due to particle presence show that inertial effects dominate particle behavior in PV panel wakes. Furthermore, the rotational behavior of tracer and particle-laden flow throughout the wake is concluded to be scale-dependent. This study has major implications for further research, both in soiling mechanics for large-scale PV systems and toward fundamental understanding of inertial particle motion in asymmetric, bluff body wakes. As multi-phase wake studies on inclined plates had been previously limited to primarily numerical simulations, and as inertial particle dynamics have shown to correlate with turbulent wake modification, this

study is strong motivation for discovering the role of preferential concentration leading to panel soiling and impact loading. The time-solved data can give insight into vortical structures and relevant frequencies.

REFERENCES

- Chen, Jerry M. & Fang, Yuan-Cheng 1996 Strouhal numbers of inclined flat plates. *Journal of Wind Engineering and Industrial Aerodynamics* **61** (2), 99–112.
- Ferran, Amélie, Machicoane, Nathanaël, Aliseda, Alberto & Obligado, Martín 2023 An experimental study on the settling velocity of inertial particles in different homogeneous isotropic turbulent flows. *Journal of Fluid Mechanics* **970**, A23.
- Glick, Andrew, Smith, Sarah E., Ali, Naseem, Bossuyt, Julian, Recktenwald, Gerald, Calaf, Marc & Cal, Raúl Bayoán 2020a Influence of flow direction and turbulence intensity on heat transfer of utility-scale photovoltaic solar farms. *Solar Energy* **207**, 173–182.
- Miller, David C., Muller, Matt T. & Simpson, Lin J. 2016 Review of artificial abrasion test methods for pv module technology. *Tech. Rep.*. National Renewable Energy Laboratory (NREL).
- Mora, D. O., Muñoz Pladellourens, E., Riera Turró, P., Lagauzere, M. & Obligado, M. 2019 Energy cascades in active-grid-generated turbulent flows. *Physical Review Fluids* **4**, 104601.
- Moutinho, H.R., Jiang, C.-S., To, B., Perkins, C., Muller, M., Al-Jassim, M.M. & Simpson, L. 2017 Adhesion mechanisms on solar glass: Effects of relative humidity, surface roughness, and particle shape and size. *Solar Energy Materials & Solar Cells* **172**, 145–153.
- Rafkin, S., Jemmett-Smith, B., Fenton, L., Lorenz, R., Takemi, T., Ito, J. & Tyler, D. 2016 Dust devil formation. *Space Science Reviews* **203** (1), 183–207.
- Said, S.A.M. 1990 Effects of dust accumulation on performances of thermal and photovoltaic flat-plate collectors. *Applied Energy* **37** (1), 73–84.
- Smith, Sarah E., Djeridi, Henda, Calaf, Marc, Cal, Raúl Bayoán & Obligado, Martín 2023 Particle transport-driven flow dynamics and heat transfer modulation in solar photovoltaic modules: Implications on soiling. *Solar Energy* **265**, 112084.
- Janiere Silva de Souza, José, Marques de Carvalho, Paulo Cesar & Barroso, Giovanni Cordeiro 2022 Analysis of the Characteristics and Effects of Soiling Natural Accumulation on Photovoltaic Systems: A Systematic Review of the Literature. *Journal of Solar Energy Engineering* **145** (4), 040801.
- Stanislawski, Brooke J., Harman, Todd, Silverman, Timothy J., Cal, Raúl Bayoán & Calaf, Marc 2022 Row spacing as a controller of solar module temperature and power output in solar farms. *Journal of Renewable and Sustainable Energy* **14** (6), 063702.
- Thornton, J.P. 1992 The effect of sandstorms on PV arrays and components. In *Solar World Congress*, pp. 13–18.
- USDA 2012 Engineering Classification of Earth Materials. In *National Engineering Handbook*. U.S. Department of Agriculture Natural Resources Conservation Service.
- Zaihidee, Fardila Mohd, Mekhilef, Saad, Seyedmahmoudian, Mehdi & Horan, Ben 2016 Dust as an unalterable deteriorative factor affecting PV panel's efficiency: Why and how. *Renewable and Sustainable Energy Reviews* **65**, 1267–1278.